

HYBRID RADIATION MODES OF MICROWAVE INTEGRATED CIRCUIT (MIC) LINES — THEORY AND APPLICATION

W. Zieniutycz

Gdańsk University of Technology
Faculty of Electronics, Telecommunications and Informatics
Narutowicza 11/12, 80-952 Gdańsk, Poland

Abstract—Spectral domain approach for continuous spectrum of wide class of microwave integrated circuit (MIC) lines is proposed. The continuous spectrum is treated as a continuum of so called hybrid radiation modes. They are the limits of volume modes of line in which lower and/or upper shieldings are moved to infinity. In the preliminary part of analysis a convenient classification of MIC lines into one-side opened and two-sides opened lines is introduced. The spectral domain representation of hybrid radiation modes is discussed in detail and boundary conditions for visible and invisible parts of spectrum are formulated. The normalization conditions in spectral domain are also proposed for both classes of lines. In the next part of paper an iterative approach in spectral domain is proposed for hr modes of one-side opened line. The boundary conditions for hybrid radiation modes are combined with spectral domain approach and the second order equation is formulated for unknown spectral amplitudes of electric or magnetic fields in visible part of spectrum. Two schemes of iteration are presented and they both lead to solutions classified as hybrid $\text{EH}^{(y)}$ and $\text{HE}^{(y)}$ modes. In the case of two-sides opened lines the solution is a sum of two partial solutions corresponding to symmetrical and unsymmetrical sources distributions. Each partial solution can be found by the iterative procedure proposed for one-side opened lines. The efficiency of proposed procedure was verified for the case of hybrid radiation modes of microstrip line. The results of calculations of amplitudes and phases of spectral amplitudes in visible spectrum part for exemplary hybrid radiation modes are shown. As an example of an application of the hybrid radiation modes concept, the advanced cavity model of rectangular patch antenna is proposed. This model allows to calculate the parameters with acceptable precision nearly ten times faster than professional full-wave design tools. In the

conclusion other possible applications of this approach are proposed e.g., in modal analysis of discontinuities including the radiation effect or 3D rectangular patch analysis.

1. INTRODUCTION

The radiation from microwave integrated circuit (MIC) and millimetre microwave integrated circuits (MMIC) waveguiding structures is interesting in both its theoretical and practical aspects. It is caused by the fact that this phenomenon cannot be neglected in many practical cases so its exact description is necessary to anticipate the properties of open structures. It is a well known fact [1] that the radiation from the dielectric slab waveguide can be represented by the continuum of the TE and TM *radiation modes*. Radiation modes are orthogonal mutually as well as they are orthogonal to the surface waves, which form the discrete part of slab waveguide spectrum. In the case of microstrip or slot-like lines simple representation in form of TE and TM modes is not valid so during the last decades different approaches have been proposed to describe more or less exactly the radiation effect.

The first group of methods approached the radiation as a continuum of the modal functions. M. Davidovitz [2] proposed such functions for air slot-line in the elliptical coordinate system. To find the modal function for dielectric microstrip line T. Rozzi and G. Cerri [3] applied LSM and LSE representation. Another approach has been proposed in [4] for layered slot-line. The authors adopted spectral domain approach (SDA) to the case of radiation modes. They introduced the *continuous modes* which were the effects of the illuminations of the line from both sides by TE and TM waves.

Second group of the methods applied the concept of leaky waves to describe the radiation from an open waveguide. The complex phase constant $k_z = \beta - j\alpha$, $\alpha \neq 0$ was introduced in lossless open line in order to simulate the radiation. Leaky wave does not fulfil the radiation condition but it can be used to describe partially the effect of the radiation loss. The concept of application of leaky waves arose from the suitable deformation of integration path during the implementation the saddle point method in asymptotic calculation of total field around the line. The choice of different paths of integration in complex plane of transversal phase constant can lead to the solutions [5, 6] which describe the different mechanisms of losses (e.g., surface wave loss, space wave loss or volume wave loss in the case of covered line).

There is also another group of methods in which the loss for radiation are calculated indirectly. P. B. Katehi [7] solved Poynting equation for open microstrip line and found the standing

wave distribution. Afterwards the complex reflection coefficient were determined and the radiation conductance of open end of the microstrip. In another approach total radiation loss of open discontinuities is found by integration of Poynting vector of far field. The loss for surface waves are calculated as the residues of the integral over side wall of cylinder surrounding the discontinuity [8]. T. K. Sarkar et al., proposed the application of Matrix Pencil Approach [9,10] to decompose the current distribution on the structure in a forward and backward waves as well as the higher modes. The S-parameters was obtained from modal amplitudes of incident and reflected waves so the radiation loss could be evaluated from unitary properties of S-matrix for a lossless structure.

Recently an interesting method of analysis of the different types of losses was presented in papers [11,12]. The authors used delta-gap feed on the microstrip line and transformed it (via Fourier transform) in longitudinal direction. This process decomposed the source into infinite set of the phased line sources. For each source Green function was found by solving the integral equation. The strip current could be then calculated by the inverse transform and different choice of the integration along the longitudinal phase constants led to different solutions. Thus the contributions of each type of the leakage could be calculated.

As a conclusion we can notice that an analysis of radiation from open MIC structures seems to be still attractive and interesting for microwave researchers' and engineers' communities.

In this paper an unified SDA approach for continuous spectrum (CS) of multilayered strip- and slot-like transmission lines is proposed. CS is treated as a continuum of *hybrid radiation modes* (hr modes) which are the limits of volume modes of shielded line when the shielding recedes to infinity. In Section 2, a convenient classification of MIC lines from the point of view of CS analysis introduced. There are defined one-side opened and two-sides opened MIC lines. For each class the cross section of the lines is divided into two parts: *the core* and *the periphery*. The fundamental properties of spectral representation of hr mode are also discussed in this section. It is shown that the verification of the condition at infinity for hr mode [14] at the periphery of the line leads to different conditions for visible and invisible parts of spectrum. The SDA for one-side opened line is presented in Section 3. An iterative procedure is proposed to solve the set of the functional equations together with condition at infinity for hr mode. Two schemes of iteration are proposed. The criterion of proper choice of the scheme is the condition of finite power flux. Section 4 describes the approach for two-sides lines. The convergence of the proposed iterative procedure

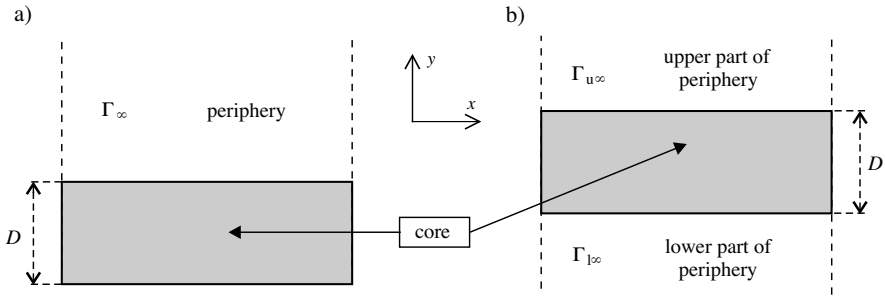


Figure 1. One-side opened (a) and two-sides opened (b) MIC lines.

was tested and confirmed for exemplary case of microstrip line. The results of calculation are shown in Section 5. An example of an application of specific hr mode with phase constant $\beta \approx 0$ is a cavity model of rectangular patch antenna presented in Section 6. The results of calculations of the resonant frequencies and radiation resistances are shown and compared with available data and results obtained from commercial 2D+ and 3D simulators showing the important gain in time of calculation. The radiation pattern is also calculated and compared with data obtained from other approaches. The final part of the paper contains the concluding remarks and the perspectives of the approach.

2. SPECTRAL DOMAIN REPRESENTATION OF HR MODES IN ONE-SIDE AND TWO-SIDES OPENED MIC LINES

Presently many different planar lines are used in the microwave technique. They are classified using criteria such as the number of strips, slots, presence or absence of ground plane or mechanism of coupling. In the case of continuous spectrum analysis it seems reasonable to introduce another classification which permits to unify the analysis. We propose to define two classes of MIC lines: *one-side opened* and *two-sides opened* lines. The cross sections of the lines are shown in Fig. 1. One-side opened lines are defined as MIC lines which are shielded from the bottom by the perfectly reflecting wall (in practice it is the electric wall). All microstrip-like MIC lines will belong to this group. The slot-like and coplanar-like lines without homogeneous shielding will be classified as two-sides opened lines. At this point we note that the side shielding is not important in this classification since we analyse the radiation effect in $\pm y$ directions. We will use spectral domain approach so the presence of the side shielding

will result in application of discrete Fourier transform.

The classification we propose permits to divide the cross section of the lines into two parts: *the core* and *the periphery* of the line. The core of the line consists of dielectric layers and the strips and/or slots placed in the interfaces between them or/and on the top/bottom of the core. The core of the one-side opened line is then limited from the bottom by the shielding whereas the two-sides lines is not limited.

The periphery Γ of the line is defined as an unbounded region:

- above the core in one-side opened line (Γ_∞),
- above and below the core in two-sides opened line

As a consequence the periphery of two-sides opened line consists of lower ($\Gamma_{l\infty}$) and upper ($\Gamma_{u\infty}$) parts.

Now we consider the field representation of hr mode in the core and in the periphery of any of the defined MIC lines. Let us remind that hr mode is the limit case of the volume mode of shielded line. It seems natural to apply well known elements of SDA formulated for discrete part of spectrum to CS analysis. We assume therefore (omitting the term $e^{-j\beta z}$) the Fourier transforms of longitudinal components of the electric and magnetic fields of single hr mode in the periphery in the form:

$$\left\{ \begin{array}{l} E_{zi}(\alpha, y) \\ \eta H_{zi}(\alpha, y) \end{array} \right\} = \left\{ \begin{array}{l} A_{Ei}(\alpha) \\ A_{Hi}(\alpha) \end{array} \right\} e^{-j\gamma_i y} + \left\{ \begin{array}{l} B_{Ei}(\alpha) \\ B_{Hi}(\alpha) \end{array} \right\} e^{j\gamma_i y} \quad (1)$$

where: $\gamma_i = \sqrt{\rho_i^2 - \alpha^2}$, α - transform variable, $\rho_i^2 = k_0^2 - \beta^2$, $i = \Gamma_{l\infty}$ lub $\Gamma_{u\infty}$ correspond to lower and upper peripheries of the line. Normalizing coefficient η is equal $-j120\pi$ [Ω]. In the case of one-side opened line we will omit the indices u and l .

From physical point of view relation (1) represents a sum of incoming and outgoing y -direction waves. The presence of both waves in representation (1) is necessary since hr mode "feels" the electric wall in infinity [1]. From mathematical point of view the presence of both waves can be explained with a help the Sturm-Liouville (S-L) operator theory. For open MIC lines we have singular endpoints ($y \rightarrow \pm\infty$) and it results in nonself-adjoint S-L problem [13]. In such case we construct the solution as a sum of the eigenfunctions for given problem (outgoing wave) and the eigenfunctions of the adjoint problem (incoming wave).

We should emphasize that representation (1) concerns single hr mode. It can be propagating mode (β - real, $\beta \in (0, k_0)$) or cut off mode (β - imaginary, $j\beta \in (-j\infty, j0)$). Total continuous spectrum is the sum of the continua mentioned above.

Representation (1), should verify the condition to be limited at infinity according to [1]. As a consequence the spectral amplitudes

in (1) should show different behaviour in visible and invisible parts of Fourier spectrum. It leads to different conditions which should be imposed on spectral amplitudes. In the invisible region of spectrum ($|\alpha| > \rho_\Gamma$, $\alpha \in \mathbf{R}$) we get:

- for one-side opened line:

$$A_{E\Gamma\infty}(\alpha) = A_{H\Gamma\infty}(\alpha) = 0 \quad (2)$$

- for two-sides opened line:

$$A_{E\Gamma u\infty}(\alpha) = A_{H\Gamma u\infty}(\alpha) = 0 \quad (3)$$

$$B_{E\Gamma l\infty}(\alpha) = B_{H\Gamma l\infty}(\alpha) = 0 \quad (4)$$

In the visible region of spectrum ($|\alpha| < \rho_\Gamma$, $\alpha \in \mathbf{R}$) we propose to apply the condition at infinity for hr modes [14]. We obtain:

- for one-side opened line:

$$A_{E\Gamma\infty}(\alpha)B_{H\Gamma\infty}(\alpha) + A_{H\Gamma\infty}(\alpha)B_{E\Gamma\infty}(\alpha) = 0 \quad (5)$$

- for two-sides opened line:

$$A_{E\Gamma u\infty}(\alpha) \cdot B_{H\Gamma u\infty}(\alpha) + A_{H\Gamma u\infty}(\alpha) \cdot B_{E\Gamma u\infty}(\alpha) = 0 \quad (6)$$

$$A_{E\Gamma l\infty}(\alpha) \cdot B_{H\Gamma l\infty}(\alpha) + A_{H\Gamma l\infty}(\alpha) \cdot B_{E\Gamma l\infty}(\alpha) = 0 \quad (7)$$

In order to normalize the z -direction power flux of hr mode we take into account only this part which passes across the periphery — the core of the line has limited dimension so its power flux tends to zero as compared to finite power flowing by the periphery. From Parseval theorem we can calculate in spectral domain the power flux I_β for hr mode having phase constant β . We obtain for one-side opened line:

$$I_\beta = \frac{2\pi\omega\epsilon_0}{\rho_\Gamma^2} \left[\beta^* \int_0^{\rho_\Gamma} |A_{H\Gamma\infty}(\alpha)|^2 d\alpha + \beta \int_0^{\rho_\Gamma} |A_{E\Gamma\infty}(\alpha)|^2 d\alpha \right] \quad (8)$$

where $\rho_\Gamma^2 = k_0^2 - \beta^2$ and the asterisk denotes the complex conjugate value.

In the case of two-sides opened lines we assume that upper and lower parts of periphery are filled with air so the following formula is valid:

$$I_\beta = \frac{2\pi\omega\epsilon_0}{\rho_\Gamma^2} \left[\beta^* \int_0^{\rho_\Gamma} (|A_{H\Gamma u\infty}(\alpha)|^2 + |B_{H\Gamma u\infty}(\alpha)|^2 + |A_{H\Gamma l\infty}(\alpha)|^2 + |B_{H\Gamma l\infty}(\alpha)|^2) d\alpha + \beta \int_0^{\rho_\Gamma} (|A_{E\Gamma u\infty}(\alpha)|^2 + |B_{E\Gamma u\infty}(\alpha)|^2 + |A_{E\Gamma l\infty}(\alpha)|^2 + |B_{E\Gamma l\infty}(\alpha)|^2) d\alpha \right] \quad (9)$$

Concerning normalizing formulas two remarks can be formulated:

- proper behaviour of the spectral amplitudes at the limit points $\alpha = 0$ and $\alpha = \rho_\Gamma$ is necessary to assure the finite z -direction power flux. This problem will be discussed in the next sections,
- the power flux is real for propagating hr modes (β – real) and imaginary for cut off modes (β – imaginary). This fact should be taken into account in order to normalize the power flux properly.

3. ITERATIVE APPROACH IN SPECTRAL DOMAIN FOR HR MODES OF ONE-SIDE OPENED LINES

After having defined all necessary boundary conditions and normalisation formulas for hr mode we can apply them to formulate the problem in a way similar to the SDA for discrete spectrum (bounded modes). We introduce the iterative approach for simplified case of one-side opened line in which the single strip is placed at the interface the core-periphery (Fig. 2).

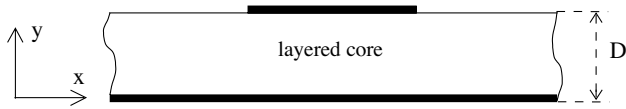


Figure 2. One-side opened line with a single strip in the core-periphery interface.

It should be emphasized that this case is easily extended for a class of practical structures which contain a combination of the strips at the different planes of the core. In SDA the change of the set of basis functions is only necessary to take into account different structure of strips. The transfer matrix concept can be used to describe the layered structure of the core.

At the first step of our approach we introduce the transforms of longitudinal components of hr modes in all layers of the core and in the periphery. Next we apply the continuity conditions at the interfaces inside the core and in the core-periphery interface, separately in visible and invisible regions taking into account the condition (2). We define the transforms of the tangential components of the fields ($\tilde{\mathbf{e}}(\alpha, D)$) and currents ($\tilde{\mathbf{j}}(\alpha, D)$) at the interface where the strip is placed. As a result inhomogeneous set of linear, functional equations is obtained. It can be written in both visible and invisible regions as:

$$[G][\tilde{\mathbf{j}}] = [\tilde{\mathbf{e}}] + [\Delta][\tilde{\mathbf{a}}] \quad (10)$$

where $[G]$ is dyadic Green function and other matrices are defined as:

$$[\tilde{e}] = \begin{bmatrix} \tilde{e}_x(\alpha, D) \\ \tilde{e}_z(\alpha, D) \end{bmatrix}; \quad [\tilde{j}] = \begin{bmatrix} \tilde{j}_x(\alpha, D) \\ \tilde{j}_z(\alpha, D) \end{bmatrix}; \quad [\tilde{a}] = \begin{bmatrix} A_{E\Gamma\infty}(\alpha) \\ A_{H\Gamma\infty}(\alpha) \end{bmatrix}$$

The matrix $[\Delta]$ we will call as matrix of forcing amplitudes and it is nonzero only in visible region. Let us note that the choice of the forcing amplitude as $\delta(\alpha - \alpha')$ corresponds to the illumination of the structure by the wave propagating in the direction defined by the wavenumber $(\alpha, \gamma_\Gamma, \beta)$.

Up to this moment we did not apply the condition (5). We rearrange it to more suitable form:

$$A_{H\Gamma\infty}(\alpha) = -Q \cdot A_{E\Gamma\infty}(\alpha) \quad (11)$$

where

$$Q = \frac{q_1 \tilde{e}_z(\alpha, D) + q_2 \tilde{e}_x(\alpha, D)}{\tilde{e}_z(\alpha, D)}$$

and

$$q_1 = \frac{\beta\alpha}{\omega\mu_0\gamma_\Gamma} \quad q_2 = \frac{\rho_\Gamma^2}{\omega\mu_0\gamma_\Gamma}$$

Now we combine (10) and (11) in order to eliminate the field transforms $\tilde{e}_x(\alpha, D)$ and $\tilde{e}_z(\alpha, D)$. It yields the second order equation (for visible part of the spectrum):

$$\begin{aligned} p_{H2} [A_{H\Gamma\infty}(\alpha)]^2 + p_{E2} [A_{E\Gamma\infty}(\alpha)]^2 + p_{EH} A_{E\Gamma\infty}(\alpha) A_{H\Gamma\infty}(\alpha) \\ + p_E A_{E\Gamma\infty}(\alpha) + p_H A_{H\Gamma\infty}(\alpha) = 0 \end{aligned} \quad (12)$$

where:

$$\begin{aligned} p_{H2} &= \Delta_{22} \\ p_{E2} &= \Delta_{21} q_1 + \Delta_{11} q_2 \\ p_{EH} &= \Delta_{21} + q_1 \Delta_{22} + q_2 \Delta_{12} \\ p_E &= -q_1 (G_{21} \tilde{j}_x(\alpha, D) + G_{22} \tilde{j}_z(\alpha, D)) \\ &\quad - q_2 (G_{11} \tilde{j}_x(\alpha, D) + G_{12} \tilde{j}_z(\alpha, D)) \\ p_H &= -G_{21} \tilde{j}_x(\alpha, D) - G_{12} \tilde{j}_z(\alpha, D) \end{aligned}$$

It is worth mentioning that generally two solutions of Eq. (12) are possible. In the absence of conducting strips the solution for multilayered dielectric waveguide consists of LSM and LSE radiating modes [15]. If we introduce conducting strips “pure” LSM and LSE modes cannot be excited — we expect y -direction hybrid modes which can be treated as perturbed $E^{(y)}$ and $H^{(y)}$ radiating modes. We will denote them as $EH^{(y)}$ and $HE^{(y)}$ modes, respectively.

Before we begin to solve Eq. (12) we note that the current transforms $\tilde{j}_x(\alpha, D)$ and $\tilde{j}_z(\alpha, D)$ depend on the spectral amplitudes $A_{H\Gamma\infty}(\alpha)$ and $A_{E\Gamma\infty}(\alpha)$. It suggests that iterative approach can be used to solve efficiently Eqs. (12) and (10). The form of (12) shows that two alternative formulations are possible:

- we treat spectral amplitude $A_{E\Gamma\infty}(\alpha)$ as an unknown function. This formulation will be called $\{H \rightarrow E\}$,
- we treat spectral amplitude $A_{H\Gamma\infty}(\alpha)$ as an unknown function. This formulation will be called $\{E \rightarrow H\}$.

We rearrange the second order Equation (12) to the product form:

$$\begin{aligned} & [A_{X\Gamma\infty}(\alpha) - f_1(A_{X\Gamma\infty}(\alpha), A_{Y\Gamma\infty}(\alpha))] \cdot \\ & [A_{X\Gamma\infty}(\alpha) - f_2(A_{X\Gamma\infty}(\alpha), A_{Y\Gamma\infty}(\alpha))] = 0 \end{aligned} \quad (13)$$

where the indices $\{X, Y\}$ correspond to:

- (i) $\{H, E\}$ – formulation $\{E \rightarrow H\}$
- (ii) $\{E, H\}$ – formulation $\{H \rightarrow E\}$.

and $f_1(A_{X\Gamma\infty}(\alpha), A_{Y\Gamma\infty}(\alpha))$, $f_2(A_{X\Gamma\infty}(\alpha), A_{Y\Gamma\infty}(\alpha))$ are known functions.

Thus in the formulation $\{E \rightarrow H\}$ spectral amplitude $A_{E\Gamma\infty}(\alpha)$ is assumed as the known function and the solutions of Eq. (13) and (10) should give the transforms of the currents and the fields corresponding to $\text{EH}^{(y)}$ and $\text{HE}^{(y)}$ modes. Iterative procedure for this formulation can be as follows:

- (i) We assume the spectral amplitude $A_{E\Gamma\infty}(\alpha)$ and the first approach of $A_{H\Gamma\infty}(\alpha)$ (e.g., zero) in the visible part of spectrum. Now we can solve Eq. (10) by moment method (in both: visible and invisible spectra) so the transforms of the currents and the fields (as well as the elements of dyadic Green function and forcing amplitudes matrix) are found,
- (ii) We solve Eq. (13) since we know all necessary coefficients p_{ij} . As a result we can find second approach of $A_{H\Gamma\infty}(\alpha)$. We introduce it to (10) and next we solve it and the second approach of the transforms of the currents and the fields is found. In such a way the iterative loop is closed.

In the case of $\{H \rightarrow E\}$ formulation the spectral amplitude $A_{E\Gamma\infty}(\alpha)$ is treated as an unknown function but the iterative procedure rests unchanged. In both formulations the unknown spectral amplitudes (functions) are defined by their values in a number of discretization

points (α_i) . Such representation is suitable for two reasons: (i) the condition of the convergence can be easily formulated for each point of discretization, (ii) the implementation of the moment method (calculation of the integrals) can be easily performed.

Some remarks concerning proposed procedure should be formulated. The first one concerns the choice of the formulations and spectral amplitude which is assumed as the known one. It is evident that the convergence should be the basic criterion and the solution should lead to the finite power flux of the mode. Second remark concerns the choice of the condition of the convergence. It can be formulated for spectral amplitude or for the transforms of the currents. The last remark concerns the method of the identification of the solutions as $\text{EH}^{(y)}$ or $\text{HE}^{(y)}$ modes. We will show in Section 5 how these problems are solved for exemplary case of microstrip line.

4. ITERATIVE APPROACH IN SPECTRAL DOMAIN FOR HR MODES OF TWO-SIDES OPENED LINES

The approach for two-sides opened lines will be discussed for the case of slot line (Fig. 3). We can formulate the problem in similar way to in the case of discrete spectrum using the procedure proposed in the previous section. However, we apply in the conditions for visible part of spectrum (6) and (7) instead of the condition (5) in this case.

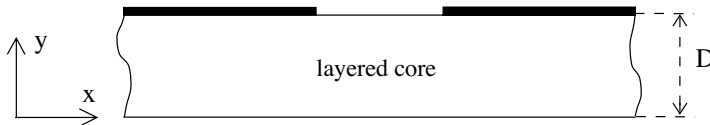


Figure 3. Two-sides opened line with a single slot in the core-periphery interface.

We start as in Section 3 from boundary conditions inside the core and in the core-periphery interface. It leads to the set of equations:

$$[G][\tilde{e}] = [\tilde{j}] + [\Delta][\tilde{a}] \quad (14)$$

where $[G]$ is dyadic Green function and matrices $[\tilde{e}]$ and $[\tilde{j}]$ are defined in the Eq. (10). Now the matrix of forcing amplitudes $[\Delta]$ has the form of column matrix:

$$[\tilde{a}] = [B_{E\Gamma l\infty}(\alpha), B_{H\Gamma l\infty}(\alpha), A_{E\Gamma u\infty}(\alpha), A_{H\Gamma u\infty}(\alpha)]^T \quad (15)$$

where the symbol T means the transpose.

Let us note that the matrix $[\Delta]$ in (15) contains four unknown amplitudes. The purpose of the next steps of the analysis is to transform Eq. (14) with conditions (6) and (7) to the form of (13) which permits to apply the iterative procedure.

In the case of two-sides opened line the periphery of the line consists of two parts so we can construct a solution as a superposition of the two partial solutions corresponding to the illumination from the lower and upper parts of periphery. Such solutions are called by C. Vasallo [16] as “regular modes”. We propose, however, an alternative formulation which permits form to transform the case of two-sides opened line into two one-side opened line cases. Our two partial solutions correspond to:

- symmetrical sources distribution:

$$A_{H\Gamma l\infty}(\alpha) = B_{H\Gamma u\infty}(\alpha) \tag{16}$$

- unsymmetrical sources distribution:

$$A_{H\Gamma l\infty}(\alpha) = -B_{H\Gamma u\infty}(\alpha) \tag{17}$$

The relation between the proposed solutions and regular modes of C. Vasallo is shown in Fig. 4.

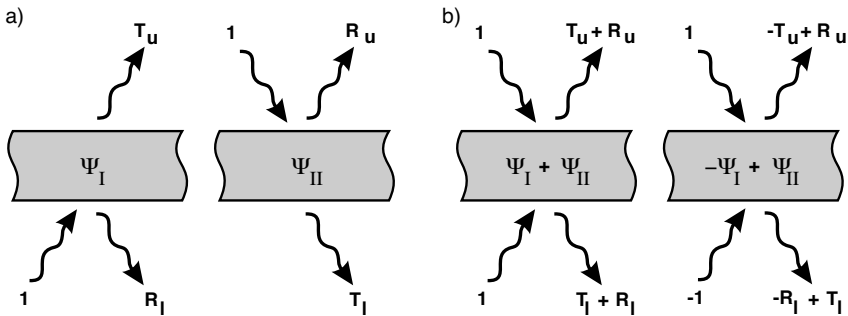


Figure 4. The relation between regular modes (a) and solutions for symmetrical and unsymmetrical sources distributions (b).

Let us note that by introducing the conditions (16) or (17) we reduce the number of unknown functions and the problem can be formulated in the same way as in the previous section. The scheme of transforming the Eq. (14) with conditions (3) and (4) to the second order equation of the form (12) will be shown for the exemplary case of $\{H \rightarrow E\}$ formulation and the symmetrical sources distribution.

We determine the spectral amplitudes in the upper part of periphery from (15) and (16):

$$A_{E\Gamma u\infty}(\alpha) = r_{00} + r_{01}B_{E\Gamma l\infty}(\alpha) + r_{02}A_{H\Gamma u\infty}(\alpha) \quad (18)$$

$$B_{E\Gamma u\infty}(\alpha) = s_{00} + s_{01}B_{E\Gamma l\infty}(\alpha) + s_{02}A_{H\Gamma u\infty}(\alpha) \quad (19)$$

Now we apply continuity conditions for tangential components of electric field at the slot interface, transfer matrix for amplitudes in the core of the line and the conditions (6) and (16). It yields the relations:

$$A_{E\Gamma u\infty}(\alpha) = r_{11}A_{E\Gamma l\infty}(\alpha) + r_{12}B_{E\Gamma l\infty}(\alpha) + r_{13}A_{H\Gamma l\infty}(\alpha) + r_{14}A_{H\Gamma g}(\alpha) \quad (20)$$

$$B_{E\Gamma u\infty}(\alpha) = s_{11}A_{E\Gamma l\infty}(\alpha) + s_{12}B_{E\Gamma l\infty}(\alpha) + s_{13}A_{H\Gamma l\infty}(\alpha) + s_{14}A_{H\Gamma g}(\alpha) \quad (21)$$

We combine (18) \div (21) and we get the relations between the amplitudes in the lower part of the periphery:

$$A_{E\Gamma l\infty}(\alpha) = r_{20} + r_{21}B_{E\Gamma l\infty}(\alpha) + r_{22}A_{H\Gamma u\infty}(\alpha) \quad (22)$$

$$A_{H\Gamma l\infty}(\alpha) = s_{20} + s_{21}B_{E\Gamma l\infty}(\alpha) + s_{22}A_{H\Gamma u\infty}(\alpha) \quad (23)$$

We introduce (22) and (23) into (7), next we apply (16) and it leads to the second order equation:

$$p_{H2}[B_{E\Gamma l\infty}(\alpha)]^2 + p_{H1}B_{E\Gamma l\infty}(\alpha) + p_{H0} = 0 \quad (24)$$

where:

$$p_{H2} = s_{21}$$

$$p_{H1} = s_{20} + A_{H\Gamma u\infty}(\alpha)(r_{21} + s_{22})$$

$$p_{H0} = r_{22}[A_{H\Gamma u\infty}(\alpha)]^2 + r_{20}A_{H\Gamma u\infty}(\alpha)$$

The coefficients r_{ij} and s_{ij} contain the current transforms $\tilde{j}_x(\alpha, D)$ and $\tilde{j}_z(\alpha, D)$ which depend on the amplitudes $B_{E\Gamma l\infty}$ and $A_{H\Gamma u\infty}$ so we can formulate Eq. (24) in the product form:

$$[B_{E\Gamma l\infty}(\alpha) - f_{1H}(B_{E\Gamma l\infty}(\alpha), A_{H\Gamma u\infty}(\alpha))] \cdot [B_{E\Gamma l\infty}(\alpha) - f_{2H}(B_{E\Gamma l\infty}(\alpha), A_{H\Gamma u\infty}(\alpha))] = 0 \quad (25)$$

It is worth mentioning that the case of unsymmetrical sources distribution does not introduce any difficulties in formulation - only the forms of coefficients r_{ij} and s_{ij} are changed. Applying the iterative procedure proposed in Section 3 we obtain the solutions corresponding to perturbed EH^(y) and HE^(y) modes. We underline that the remarks formulated in the previous section concerning the proposed iterative procedure are valid in the case of the analysis of two-sides opened line.

5. NUMERICAL RESULTS – HYBRID RADIATION MODES OF MICROSTRIP LINE

The case of one-side opened line has been analysed in order to verify the approach and a computer program was prepared. The simple structure of the microstrip line on dielectric substrate was chosen for this purpose. We should note that implementation of SDA for the discrete spectrum of this line is well known so the numerical aspects of solving of Eq. (10) will not be discussed here. Before the numerical implementation of the iterative procedure we should make some assumptions and additional considerations according to the remarks formulated at the end of Section 3.

Let us remind that in order to solve Eq. (13) we should assume the spectral amplitudes: $A_{E\Gamma\infty}(\alpha)$ or $A_{H\Gamma\infty}(\alpha)$, depending on the formulation that we have chosen ($\{E \rightarrow H\}$ or $\{H \rightarrow E\}$). As a criterion we choose the finite value of the power flux. In the discussed case of single strip according to the symmetry two solutions are possible: even ($\tilde{j}_z(\alpha, D)$ – even function of variable α) and odd ($\tilde{\tilde{j}}_z(\alpha, D)$ – odd function of variable α). To be sure that all space harmonics are present in the visible part of spectrum of hr mode we assumed:

- for even electric source:

$$A_{E\Gamma\infty}(\alpha) \sim \gamma_{\Gamma} \quad (26)$$

- for even magnetic source:

$$A_{H\Gamma\infty}(\alpha) \sim \text{const.} \quad (27)$$

Asymptotic analysis was next performed for assumed distributions (26) and (27) at the limit points $\alpha = 0$ and $\alpha = \rho_{\Gamma}$. Spectral amplitudes can be singular there and the power flux may tend to infinity according to (8). The results of analysis for different schemes and symmetries are presented in Table 1. We note that only for $\text{HE}^{(y)}$ odd mode any of the schemes leads to physical solution. In all other cases the proper choice leading to acceptable solution is unique.

In order to identify the solutions of Eq. (13) as $\text{EH}^{(y)}$ or $\text{HE}^{(y)}$ modes we used their behaviour for asymptotic values $\tilde{j} \rightarrow 0$. In this case the solutions are “pure” LSE and LSM modes for which the analytic solutions are known [14].

The last remark in Section 3 concerned the choice of the criterion of convergence. We examined this problem numerically by comparing the convergence of the coefficients of the expansion for the currents on the strip and spectral amplitudes. As a criterion of the convergence

Table 1. Asymptotic values of spectral amplitudes for $\alpha \rightarrow 0$ i $\alpha \rightarrow \rho_\Gamma$ for even and odd solutions in microstrip line on single layered dielectric substrate.

	Scheme $\{E \rightarrow H\}$				Scheme $\{H \rightarrow E\}$			
	even		odd		even		odd	
	$A_{E\Gamma\infty}(\alpha) \sim \gamma_\Gamma$		$A_{E\Gamma\infty}(\alpha) \sim \alpha \gamma_\Gamma$		$A_{H\Gamma\infty}(\alpha) \sim \alpha$		$A_{H\Gamma\infty}(\alpha) \sim \text{const.}$	
solutions	$EH^{(y)}$	$HE^{(y)}$	$EH^{(y)}$	$HE^{(y)}$	$HE^{(y)}$	$EH^{(y)}$	$HE^{(y)}$	$EH^{(y)}$
$\alpha \rightarrow 0$	α	$1/\alpha$	<i>const.</i>	<i>const.</i>	<i>const.</i>	<i>const.</i>	α	$1/\alpha$
$\alpha \rightarrow \rho_\Gamma$	<i>const.</i>	<i>const.</i>	<i>const.</i>	<i>const.</i>	γ_Γ	$1/\gamma_\Gamma$	γ_Γ	$1/\gamma_\Gamma$

Table 2. Normalised coefficients for the first basis functions of the currents $\tilde{j}_x(\alpha, D)$ (a_1) and $\tilde{j}_z(\alpha, D)$ (b_1) and the number of the points (N_+) in which the convergence criterion (28) is fulfilled. Calculations were performed for odd hr mode $EH^{(y)}$ with $\beta/k_0 = 0.5$ at the frequency $f = 15$ GHz for 495 points of discretization of the unknown spectral function and $K = 0.001$. Parameters of the line: the thickness of the substrate $D = 0.5$ mm, the strip width $2w = 3.0$ mm, the electric permittivity $\epsilon_r = 2.3$.

Number of iteration	a_1/a_5	b_1/b_5	Number of points N_+
1	$0.96441 - j0.71504 \cdot 10^{-2}$	$0.99367 - j0.69374 \cdot 10^{-3}$	0
2	$0.99874 - j0.18283 \cdot 10^{-3}$	$0.99979 - j0.95069 \cdot 10^{-5}$	0
3	$0.99998 - j0.24361 \cdot 10^{-5}$	$1.0 + j0.0$	336
4	$1.0 + j0.0$	$1.0 + j0.0$	460
5	$1.0 + j0.0$	$1.0 + j0.0$	495

we proposed a condition which should be fulfilled at each discretization point α_i :

$$\frac{|A_{X\Gamma\infty}^{(j+1)}(\alpha_i) - A_{X\Gamma\infty}^{(j)}(\alpha_i)|}{|A_{X\Gamma\infty}^{(j)}(\alpha_i)|} < K, \quad (28)$$

where X denotes E or H depending on the scheme of the iteration and indices $j + 1$ and j concern two successive iterations. The results of calculations are presented in Table 2 and they show that the criterion of convergence should be chosen for spectral amplitudes.

In fact after three iterations the coefficients of the expansion converged to their asymptotic values but criterion for spectral

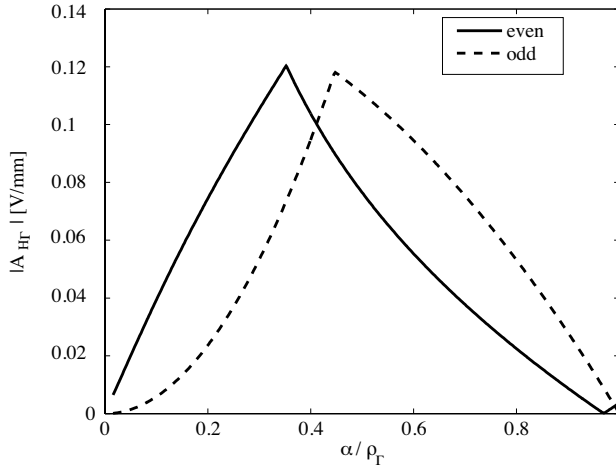


Figure 5. Module of spectral amplitudes $A_{H\Gamma\infty}(\alpha)$ for $\text{HE}^{(y)}$ modes ($\beta/k_0 = 0.5$) of microstrip line (strip width $2w = 3.0$ mm, substrate thickness $d = 1.0$ mm, $\epsilon_r = 2.3$) at the frequency $f = 3$ GHz. Solid and dashed lines concern even and odd sources, respectively.

amplitudes was fulfilled only in 336 points from 495 points of discretization.

After these preliminary calculation the efficiency of iterative procedure has been tested. We examined the influence of different parameters on the convergence of the proposed procedure. We found that convergence is nearly independent of: (i) frequency, (ii) character of the mode (propagating or cut off), (iii) parameters of microstrip line (strip width, electric permittivity). Typically $2 \div 6$ iterations are necessary to finish the iterative procedure for $K = 0.001$ in all the points of discretization α_i . The time of processor is about 1.5 s for Celeron 466 MHz (for 5 basis functions for both $\tilde{j}_x(\alpha, D)$ and $\tilde{j}_z(\alpha, D)$ current expansions and about 500 points of the discretization). In the Fig. 5 and Fig. 6 the module of spectral amplitudes of $A_{H\Gamma\infty}(\alpha)$ and $A_{E\Gamma\infty}(\alpha)$ found from iterative procedure for $\text{HE}^{(y)}$ and $\text{EH}^{(y)}$ modes were shown, respectively.

It is seen that behaviour at the limit points $\alpha = 0$ and $\alpha = \rho_T$ agrees with this presented in Table 1 (exact calculation shows that for even solution $A_{H\Gamma\infty}(\alpha)$ does not tend to zero for $\alpha \rightarrow 0$). We also note that the spectral amplitudes in all visible region have not discontinuities. The phases of the spectral amplitudes are shown in Fig. 7 and Fig. 8.

Let us remind that the assumed phases of excitation (see Table 1)

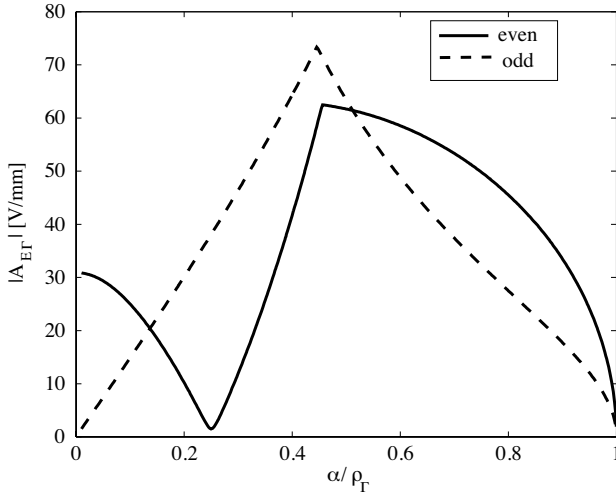


Figure 6. Module of spectral amplitudes $A_{E\Gamma\infty}(\alpha)$ for $\text{EH}^{(y)}$ mode ($\beta/k_0 = 0.5$) of the microstrip line (parameters of microstrip as in Fig. 5) at the frequency $f = 3$ GHz. Solid and dashed lines concern even and odd sources, respectively.

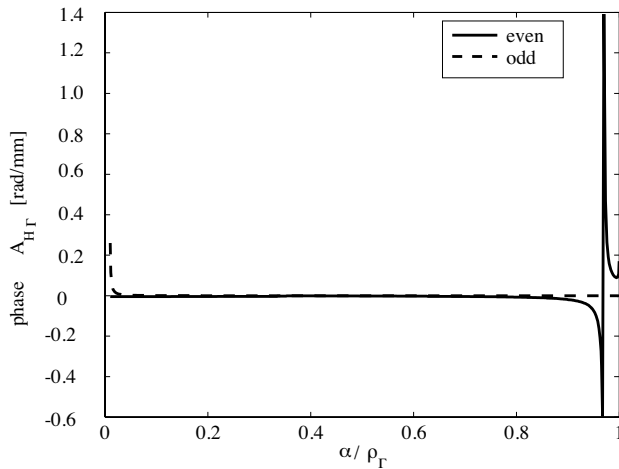


Figure 7. Phases of spectral amplitudes $A_{H\Gamma}(\alpha)$ for hr modes $\text{HE}^{(y)}$ from Fig. 5. Solid and dashed lines concern even and odd sources, respectively.

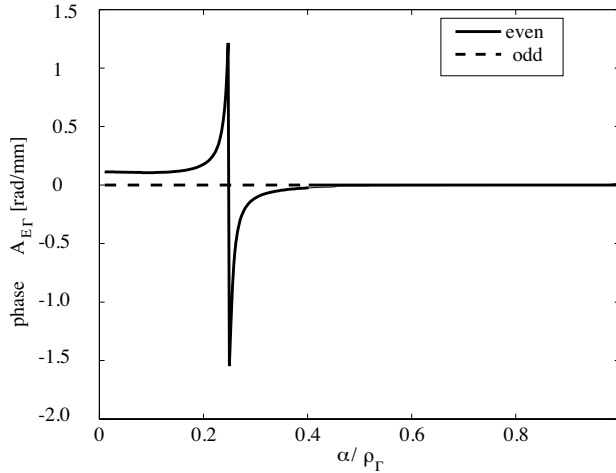


Figure 8. Phases of spectral amplitudes $A_{E\Gamma}(\alpha)$ for hr modes $\text{EH}^{(y)}$ from Fig. 6. Solid and dashed lines concern even and odd sources, respectively.

were equal zero. We observe that the phases of spectral amplitudes $A_{H\Gamma\infty}(\alpha)$ (Fig. 7) are near zero in almost whole visible region. Important changes are observed on the beginning of the region for odd source case and at the end of the region for even source case. For spectral amplitudes $A_{E\Gamma\infty}(\alpha)$ (Fig. 8) we note that the phase is near zero in all visible region for odd source case and it changes importantly only near $\alpha/\rho_\Gamma \approx 0.4$ for even source case.

6. APPLICATION – SINGLE HR MODE APPROXIMATION OF RADIATION FROM RECTANGULAR MICROSTRIP PATCH ANTENNA

Rectangular microstrip patch antenna is currently fundamental radiating element widely used in antenna technique. At present a number of full-wave models and commercial simulators are available which permit to analyse and design the antennas. However, the models which offer sufficiently good approximation of radiation and acceptable time of simulation are still interesting for researchers' and engineers' community. The proposed model is a transitory step between cavity and full-wave model and it seems to fulfill these needs.

Let us consider hr mode with phase constant $\beta \approx 0$ ($\rho_\Gamma \approx k_0$) in microstrip line.

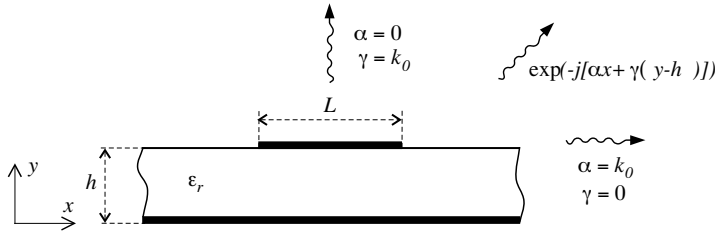


Figure 9. Cross section of microstrip line.

It is seen on Fig. 9 that such hr mode describes partial radiation from line in almost all directions of positive hemisphere $y > 0$. In fact for the lower limit of visible region $\alpha \approx 0$ wave is radiating along y axis whereas for the upper limit $\alpha \approx k_0$ it is radiating along x axis. Thus we conclude that odd $\text{EH}^{(y)}$ mode with $\beta \approx 0$ could be good approximation of $\text{TM}_{10}^{(y)}$ mode which does play fundamental role in cavity model of microstrip antenna. For this mode we can observe the current on the strip as a function of frequency. The maximum value of the current occurs for “resonant” frequency where maximum of the e-m energy is radiated from line. It is necessary to emphasize that in the case of patch antenna we should take into account its finite transversal dimension (in Fig. 9 – z direction dimension). In order to avoid this problem simple correction coefficient was proposed [17].

In Table 3 the resonant frequencies of rectangular patch antennas on thin substrate calculated by hr mode approximation are compared with results of calculation from professional simulators: MOMENTUM from ADS 2003B and QuickWave 3D v.2.2. Since the simulators were installed on different computers we used normalised times. In the case of MOMENTUM we compared the times of calculation of a single frequency point. QuickWave uses FDTD method so such comparison cannot be used. We assumed that in order to find resonant curve from hr mode approximation we need 50 frequency points so we used this value for comparison.

It is seen from Table 3 that professional simulators calculate resonant frequencies more exactly (about 1%) but at the expense of time of simulation (ten times for MOMENTUM and thirty times for QuickWave). We should note that QuickWave is time-domain simulator and antenna is narrowband so the time of the simulation can be important (for discussed case of single patch the time of processor was about 9 min. for INTEL Xeon 3 GHz). The accuracy of the approach seems to be satisfactory if we take into account the fact that electric permittivity of the substrate is often given with precision of

Table 3. Resonant frequencies and normalised times of simulations $t_{norm.}$ for rectangular patch antenna (resonant length $L = 25$ mm, antenna width $W = 40$ mm). Experimental values of resonant frequencies are taken from [18].

h/λ	Momentum		QuickWave		Hr mode approx.		Exp.
	f_0 [GHz]	$t_{norm.}$	f_0 [GHz]	$t_{norm.}$	f_0 [GHz]	$t_{norm.}$	
0.01	3.91	10	3.90	33	3.88	1	3.92
0.02	3.86	12	3.83	44	3.77	1	3.84

Table 4. Resonant frequencies (in GHz) of patch antennas on thick substrates calculated from MPM, QuickWave, hr mode approximation compared to experimental values (Exp.). Parameters of antenna substrate: thickness $h = 3.18$ mm, electric permittivity $\epsilon_r = 2.33$.

h/λ	L	W	Hr mode approx.	MPM [19]	QuickWave	Exp. [20]
0.045	19.5	29.5	4.39	4.42	4.5	4.24
0.062	13	19.5	6.3	6.31	6.34	5.84
0.088	9	14	8.7	8.3	8.38	7.7

single percents.

For antennas on thick substrates (Table 4) the differences between hr mode approximation, mixed potentials method (MPM) [19], and QuickWave results are also not important.

We observe the important differences for $h/\lambda = 0.088$. This value agrees with limit value $h/\lambda \approx 0.07$ proposed by Wood [21] (power transferred to surface waves should be less than 25% of radiated power). However other approaches differ importantly from experiment in this case. On the other hand the antennas with so thick substrates are not commonly used.

It is worth reminding that in order to find resonant frequency we calculate the resonant curve of antenna. Thus we know the quality factor of antenna so to determine the resonant resistance we need only equivalent capacitance. We propose finding it from classical dielectric filled rectangular capacitor. Effective electric permittivity which takes into account radiation effect can be defined as:

$$\epsilon_{er} = \left[\frac{f_{res}^{diel}}{f_{res}} \right]^{-2} \quad (29)$$

where f_{res}^{diel} and f_{res}^{air} correspond to the resonant frequencies of the antennas filled with dielectric and air, respectively. In Table 5 we compare resonant resistances calculated from our approach with the ones found from other full-wave approaches and experiment.

Table 5. Resonant resistances (in Ohm) for rectangular patch antennas calculated from proposed hr mode approach (R_{hrm}), from moment method (R_{MoM}) compared to the results from QuickWave (R_{Qwave}) and experiment ($R_{Exp.}$). Parameter x_f is a distance of the feeding point to radiation edge of the antenna.

Lp	L	W	h	ϵ_r	x_f	R_{hrm}	R_{MoM} [18]	R_{Qwave}	$R_{Exp.}$ [18]
1	25	40	0.79	2.22	0	111	130	151	136
2	25	40	0.79	2.22	4	86	101	88	89
3	25	40	1.52	2.22	0	122	143	136	119
4	25	40	1.52	2.22	4	94	127	60	87
5	20	30	1.27	10.2	0	196	350	445	335
6	20	30	1.27	10.2	6.5	49	100	200	85

It is seen that for lower electric permittivities the differences between our approach and experimental values differs less than 20% but they are about the same order as differences from other methods. For antennas with high electric permittivity substrates the differences are greater and proposed model cannot be accepted for practical use. However such substrates are not commonly used in antenna technique. We also note that other methods give important error for such structures.

In order to find the radiation pattern we apply the angular spectrum concept. In the case of single hr mode approximation ($\partial/\partial z \approx 0$) we assume the transforms of the currents on the strip in the form:

$$\left\{ \begin{array}{l} \tilde{j}_x(\alpha, k_z) \\ \tilde{j}_z(\alpha, k_z) \end{array} \right\} \sim \frac{\sin \frac{k_z W}{2}}{\frac{k_z W}{2}} \left\{ \begin{array}{l} \tilde{j}_x(\alpha, h) \\ \tilde{j}_z(\alpha, h) \end{array} \right\} \quad (30)$$

where current transforms $\tilde{j}_x(\alpha, h)$ and $\tilde{j}_z(\alpha, h)$ are solutions of Eq. (10), k_z is variable transform in z direction. Now we introduce (30) into (10) and we calculate electric field transforms in aperture plane $y = h$:

$$[\tilde{e}(\alpha, k_z)] = [G] [\tilde{j}(\alpha, k_z)] - [\Delta] [\tilde{a}] \quad (31)$$

The knowledge of the electric field transforms at the aperture interface $y = h$ permits to determine radiation field. In Fig. (10) we show

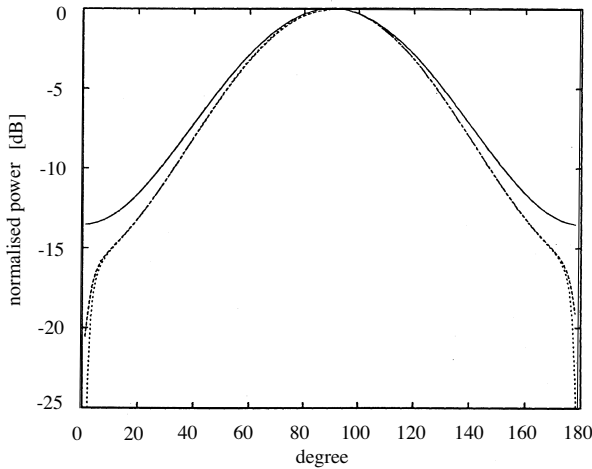


Figure 10. E-plane pattern of rectangular patch antenna calculated at the frequency $f = 3.84$ GHz. Antenna structure parameters: $L = 25$ mm, $W = 40$ mm, $h = 0.7$ mm, $\epsilon_r = 2.2$. Solid line concerns [22], dashed line hr mode approach, dotted line [23].

E-plane antenna pattern calculated for exemplary rectangular patch antenna compared with patterns found from other approaches. It is seen that the differences are generally small. More important differences are observed for the directions far from main lobe direction. In the case of H-plane pattern the differences were very small so we do not show the pattern here.

It is worth mentioning that proposed cavity model can be easily extended to the case of the coupled rectangular patch antennas. In this case the effect of mutual coupling can be examined as was shown in [17].

7. CONCLUDING REMARKS

In the paper we present a new approach for radiation modes of two classes of multilayered open MIC lines: one-side opened and two-sides opened lines. In the proposed approach a single radiation mode has a hybrid character and is treated as a volume mode of a shielded line in which the shieldings are moved to infinity. The method of evaluation of dyadic Green functions for both classes was proposed as well as the iterative procedure of solving associated boundary value problem.

The convergence of the procedure was tested and the exemplary results of calculation of the complex spectral amplitudes of perturbed $HE^{(y)}$ and $EH^{(y)}$ hr modes were shown. As an application the advanced cavity model of rectangular patch antenna was presented based on approximation of radiation field of antenna by single hr mode. The model permits to determine in reasonable time the resonant frequency, radiation resistance and radiation pattern of rectangular patch with reasonable accuracy.

It is worth mentioning that proposed approach gives the full representation of CS of radiating waves for open MIC lines. Combining CS with discrete spectrum we can perform the complete modal analysis of the radiating discontinuities. Other possible application is an extension antenna 2D approach to 2D+ approach by formulating 2D condition in infinity for hr mode. These problems are the subject of current interest of the author.

REFERENCES

1. Shevchenko, V. V., *Continuous Transitions in Open Waveguides*. Prentise Hall, Englewood Cliffs, NJ, 1973.
2. Davidovitz, M., "Continuous spectrum and characteristic modes of the slot line in free space," *IEEE Trans.*, Vol. MTT-44, No. 2, 340–341, 1996.
3. Rozzi T. and G. Cerri, "Radiation modes of open microstrip with application," *IEEE Trans.*, Vol. MTT-43, No. 6, 1364–1369, 1995.
4. Citerne, J. and W. Zieniutycz, "Spectral domain approach for continuous spectrum of slot-like transmissions lines," *IEEE Trans.*, Vol. MTT-33, No. 817–818, 1985.
5. Grim, J. M. and P. P. Nyquist, "Spectral analysis consideration relevant to radiation and leaky modes of open-boundary microstrip line," *IEEE Trans.*, Vol. MTT-41, No. 1, 150–153, 1993.
6. Das, N. K. and D. M. Pozar, "Full wave spectral-domain computation of material, radiation and guided wave losses in infinite multilayered printed transmission lines," *IEEE Trans.*, Vol. MTT-39, No. 1, 54–64, 1991.
7. Katehi, P. B. and N. G. Alexopoulos, "Frequency-dependent characteristics of microstrip discontinuities in millimeter-wave integrated circuits," *IEEE Trans.*, Vol. MTT-33, No. 10, 1029–1036, 1985.
8. Horng, T-S., S.-C. Wu, H.-Y. Yang, and N. G. Alexopoulos, "A generalized method for distinguishing between radiation and

- surface-wave losses in microstrip discontinuities," *IEEE Trans.*, Vol. MTT-38, No. 12, 1800–1807, 1990.
9. Sarkar, T. K., Z. A. Maricevic, and M. Kahrizi, "An accurate de-embedding procedure for characterizing discontinuities," *International Journal of Microwave and Millimeter-Wave Computer-Aided Engineering*, Vol. 2, No. 3, 135–143, 1992.
 10. Sarkar, T. K., Z. A. Maricevic, and M. Salazar-Palma, "Characterization of power loss from discontinuities in guided structures," *MTT-S Int. Microwave Symposium*, Vol. 2, No. 2, 613–616, 1997.
 11. Mesa, F. and D. R. Jackson, "The danger of high-frequency spurious effects on wide microstrip line," *IEEE Trans.*, Vol. MTT-50, No. 12, 2679–2690, 2002.
 12. Freire, M., F. Mesa, C. de Nallo, D. R. Jackson, and A. A. Oliner, "Spurious transmission effects due to the excitation of the bound mode and the continuous spectrum on stripline with air gap," *IEEE Trans.*, Vol. MTT-47, No. 12, 2493–2502, 1999.
 13. Hanson, G. W. and A. B. Yakovlev, *Operator Theory for Electromagnetics — An Introduction*, Springer-Verlag, New York, 2002.
 14. Zieniutycz, W., "A new formulation of boundary condition at infinity for hybrid radiation modes and its application to the analysis of radiation modes of microstrip lines," *IEEE Trans.*, Vol. MTT-38, No. 9, 1294–1299, 1990.
 15. Felsen, L. B. and N. Marcuvitz, *Radiation and Scattering of Waves*, Prentice-Hall Inc., New Jersey, 1973.
 16. Vasallo, Ch., *Théorie des Guides d'ondes Électromagnétiques*, Eyrolles, Paris, 1985.
 17. Zieniutycz, W., "Application of hybrid radiation modes of microstrip line in the design of rectangular microstrip antennas," *IEE Proc. — Microw. Antennas Propag.*, Vol. 145, No. 5, 421–423, 1998.
 18. Schaubert, D., D. Pozar, and A. Adrian, "Effect of microstrip antenna substrate thickness with experiments," *IEEE Trans.*, Vol. AP-37, No. 5, 677–682, 1987.
 19. Hall, R. C. and J. R. Mosig, "The analysis of coaxially fed microstrip antennas with electrically thick substrates," *Electromagnetics*, Vol. 9, 367–384, 1989.
 20. Hang, E., S. A. Long, and W. F. Richards, "Experimental investigation of electrically thick rectangular microstrip antennas," *IEEE Trans.*, Vol. AP-34, 767–772, 1986.

21. Wood, C., "Analysis of microstrip circular patch antennas," *IEE Proc.*, Vol. 128H, 69–76, 1981.
22. Thouroude, D., M. Himdi, and J. P. Daniel, "CAD-oriented cavity model for rectangular patches," *Electron. Lett.*, Vol. 26, No. 13, 842–844, 1990.
23. Jackson, P. R. and T. R. Williams, "A comparison of CAD models for radiation from rectangular microstrip patch," *Int. Journal of Microw. and Millimeter-Wave Computer-Aided Engineering*, Vol. 1, No. 2, 236–245, 1991.